33rd Annual International Conference of the IEEE EMBS
Boston, Massachusetts USA, August 30 - September 3, 2011

Integrated Heaters for Temperature Control in Disposable Bioassay Cartridges for Use with Portable, Battery-Operated Instruments

Luis Ortiz Hernandez, *Member, IEEE*, Haile Negussie, Laura T. Mazzola, Daniel J. Laser, and Amy Droitcour, *Member, IEEE*

***Abstract*—Two methods for heating fluids in microliter- to milliliter-scale reaction chambers in disposable bioassay cartridges are analyzed and compared. Inductive heating requires no electrical contact between the energy source and the cartridge and uses a very inexpensive component in the cartridge. Resistive heating with a surface mount component requires electrical interconnection, but is generally conducive to low-cost off-the-shelf components. Typical power consumption for both inductive heating and resistive heating is consistent with battery-powered operation. A finite element model for heating an injection-molded plastic cartridge with a surface-mount resistor has been developed and validated through experiments on a 40 mm x 10 mm x 7.5 mm injection molded polystyrene cartridge with embedded 1kΩ surface-mount resistors. A model of frequency-dependent heat generation in a novel inductive heating device is also presented.**

I. Introduction

HEATING of samples and reagents is required in both nucleic acid and antibody assays for many kinds of *in vitro* diagnostics. Temperature control is used to increase diffusion, to selectively promote specific binding over non-specific binding, and to increase signal output. In resource-limited settings, where the assay is conducted in ambient temperatures ranging from 20-30°C [1-3], temperature control is also important to improve reproducibility of assays that have been validated at room temperature in climate-controlled settings [4-7].

For most high-throughput microarray or microwell clinical diagnostics, heating is conducted with a plate heater or a heated plate reader, both of which use large resistive heaters that operate on wall power. Microfluidic diagnostics for point-of-care use generally require lower power consumption. Most methods achieve low power consumption by locally heating the chamber in which the small sample resides.

Many heating methods have been developed for chip-based polymerase chain reaction (PCR) assays, but these methods are typically focused on reducing the time constant for temperature cycling, which limits the time in which PCR is complete. When designing heaters for isothermal assays, temporal response is a less critical parameter, whereas other parameters such as size, power consumption, thermodynamic efficiency, spatial effects, and part-to-part reproducibility in mass production may be more critical.

The most widely applied methods for temperature control of PCR microfluidics are thin film heating elements (mostly platinum or polysilicon), metal heating blocks, and Peltier-effect-based thermo-electric ceramic heating blocks [8]. Other methods that have been used for PCR microfluidics include commercial thin film resistance heaters on flexible printed circuits, resistive heater coils, hot air cycling, infrared light radiation, induction heating, microwave radiation, running an electric current through the buffer in the assay solution, and external water baths [8,9]. Several devices designed for use in resource-limited settings use exothermic chemical reactions for heat [10-13].

While many PCR-based detection schemes require rapid thermal cycling between 55 and 95°C [14,15] , many ELISA (enzyme-linked immunosorbent assay), signal amplification [16,17], and isothermal nucleic acid amplification assays [8,18-21] require holding a constant temperature between 30 and 70°C for 10 minutes to 8 hours. Additionally, many of the chip-based PCR devices are designed on silicon or glass [15,22], while low-cost microfluidic cartridges for diagnostics in resource-limited settings can be made with plastics in an inexpensive injection-molding process.

This paper describes the evaluation of heaters that can be integrated in an injection-molded plastic microfluidic cartridge to heat assay reagents and hold them at a constant temperature. Key parameters for evaluation of heaters for these devices include efficiency, cost of components, simplicity of interface to driving electronics, and ease of assembly/manufacturability. This work will focus on heaters consistent with holding assay reagents at a constant temperature, and not on rapid temperature cycling for PCR.

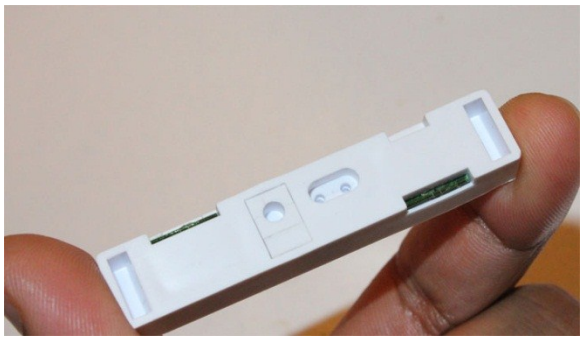

Figure 1. Wave 80 Biosciences EOSCAPE disposable assay cartridge.

Disposable cartridges used in emerging commercial bioassay systems, such as the nucleic acid blood test cartridge pictured inFigure 1, incorporate heaters to

Manuscript received April 15, 2011. This work was supported in part by the
Luis Ortiz Hernandez, Haile Negussie, Laura Mazzola, Daniel J. Laser and Amy Droitcour are with Wave 80 Biosciences, Inc. San Francisco, CA 94107 USA. (415)-487-7976; e-mails: luis.ortiz@wave80.com, haile.negussie@wave80.com, laura.mazzola@wave80.com daniel.laser@wave80.com, amy.droitcour@wave80.com.

selectively control cartridge temperatures along with sub-centimeter-scale low-cost microactuator chips to drive sample and reagent transport. With all reagents held onboard the cartridge and fluidic actuation accomplished through direct transduction of electrical power into fluid power, failure modes associated with cartridge-instrument fluidic interconnects or with mechanical actuator interfaces are eliminated. Assay process automation within disposable cartridges enables a one patient-one test usage model, while engineered fluidic processes enhance assay performance and reduce overall turnaround time. Configuring all components that contact infectious material within a disposable cartridge minimizes the risk of infectious disease transmission to health care workers.

Heating methods appropriate for bioassay cartridges similar to that in Figure 1 include patterned film resistive heaters, carbon ink printed resistive heaters, optically heating an absorptive material, joule heating of fluid, inductively heating a conductive material, and resistively heating a surface mount resistor. Inductive heating and resistive heating have many inherent advantages for disposable bioassay cartridges. Non-contact inductive heating only requires a piece of a magnetic and conductive material to be insert-molded into the cartridge, and no electrical connections to this material are required, which keeps the manufacturing complexity and cost low. Resistive heating is a well-established method (although not with surface-mount resistors), and because a PCB is already required to provide connection to the electroosmostic microchips in the cartridge, including surface-mount resistors on the cartridge PCB adds minimal cost to the manufacturing process. The power consumption of both of these methods is consistent with battery operation. Neither method is likely to directly affect the sample or to cause steam or bubbles that may affect the bioassay or operation of the microfluidics.

II. Numerical Modeling of Resistive Heating of Fluid in Cartridge Well

A. Model of Surface Mount Resistor and Cartridge

A 3mm-diameter 35uL well in a high impact polystyrene (HIPS) injection-molded cartridge was used as a model system for evaluation of heating methods. To investigate the effects of heating resistor selection, cartridge geometry, material properties, and other engineering design parameters, the design was simulated with both stationary and time-dependent finite-element simulations in COMSOL™ Mutiphysics Modeling and Simulation Software. In this simulation, heat transfer and Joule heating physics are utilized.

Joule heating is the process by which electrical current flowing through a resistive element dissipates heat. The instantaneous heat is dissipated at a rate *P(t)* (W) of:

$$P(t) = R \cdot i(t)^2 \quad (1)$$

with a total heat generated of:

$$Q = \int_{t1}^{t2} R \cdot i(t)^2 dt \quad (2)$$

where *R* is the electrical resistance of the material (Ω), *i(t)* is the time-varying electrical current (A), *Q* is the total heat dissipated (J), and *t1* and *t2* are the start and stop times over which the heat is measured (s) [23].

Heat transfer models are used to determine temperature changes in the fluid as a function of time. With Joule heating of the resistor as the heat source, heat is transferred into the plastic cartridge and in turn into the fluid phase contained within the cartridge fluid passageways and reservoirs. The following heat conduction equation is used:

$$\nabla^2 T + \frac{q_{gen}}{K} = \frac{\rho c}{K}\frac{\delta T}{\delta t} \quad (3)$$

where *T* is the temperature as a function of location and time (K), q_{gen} is the heat generated per unit volume (J/m^3), *K* is the thermal conductivity of the material (W/(m· K)), ρ is the mass density of the material (kg/m^3), *c* is the specific heat of the material (J/(g·K)), and *t* is time (s) [24].

The cartridge is simulated as a 40mm x 7.5mm x 10mm polystyrene block with a 3mm diameter x 5mm well, and two rectangular cutouts for moldability, as shown in Figure 2. The well (the top of the two blue highlighted sections in the figure) is filled with a homogenous fluid phase with physical properties taken as those of water at room temperature. A 4mm diameter cavity (the bottom blue highlighted section), of varying depth, is formed in the bottom of the cartridge, directly below the well. The heating resistor is situated within this cavity at the point of closest proximity to the well. The heating resistor makes direct physical contact with the plastic, and all extra volume of the heating-resistor cavity is filled with conductive paste. The resistor is 3.2mm x 0.55mm x 1.6mm (consistent with a 1206 resistor package) with a resistance value of 1kΩ.

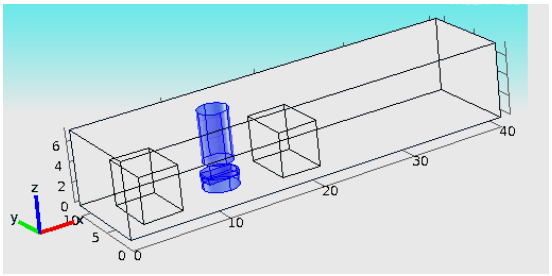

Figure 2. Cartridge geometry for COMSOL simulation. The well for the fluid phase and the cavity formed for the heating resistor are highlighted in blue. Dimensions are in mm.

Initial temperature and voltage values are set at 298K and 0V, respectively. At the beginning of the simulation, the voltage across the resistor was set to 15V.

To simplify the model, convective heat transfer analysis in the fluid phase was excluded from the simulation. Instead, fluid phase conductive heat transfer was modeled with a heat transfer coefficient of zero, minimizing temperature nonuniformity within the well. As discussed later, comparison with physical experiments affirmed this assumption to be reasonable for purposes of bioassay cartridge modeling. Thermal conductivity, density, and specific heat parameters of the materials used in the simulation are listed in Table 1.

TABLE I
PARAMETRIC VALUES FOR COMSOL SIMULATION

Material	Thermal Conductivity (W/(m·K))	Density (kg/m^3)	Specific Heat (J/(kg·K))
Water	0.481	980	4185
Polystyrene	0.04	16	1210
Resistor	100	8900	445
Conductive Paste	1000	10,000	1

W=watts, m=meters, kg=kilograms, J=Joules, K=Kelvin

Resistor (values given are for 80% Ni, 20% CR NiChrome), Polystyrene (values given are for molded beads), and water values are from [24][24]. Conductive Paste information is from Arctic Silver, manufacturer of the paste used in the experiment [25].

B. Analysis of Plastic Thickness between Resistor and Well

To determine the sensitivity of the system's thermal response to the distance between the heating resistor and the bottom of the well, three different designs were simulated with l_g at 100, 300, and 600 µm. (The parameter l_g is defined in Figure 3.) While minimizing l_g can be expected to result in the fastest well temperature response, mapping the functional relationship between l_g and heating performance provides important input for design-for-manufacturability analysis.

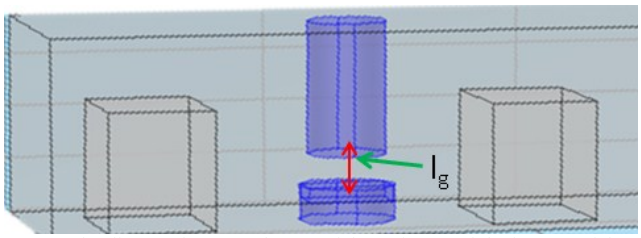

Figure 3. The distance between the top of the resistor and the bottom of the well, l_g, was simulated at different distances.

III. THEORY OF INDUCTIVE HEATING OF FLUID IN CARTRIDGE WELL

Inductive heating involves generating an electromagnetic field that transfers energy to a conductive material that is not in contact with the generator. The induced energy generates a current in the conductive material that is transformed into heat via the Joule effect. Figure 4 depicts the basic blocks in the inductive heating system developed in this work.

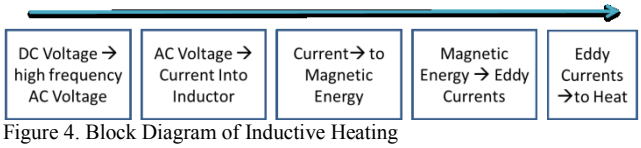

Figure 4. Block Diagram of Inductive Heating

A circuit converts DC battery voltage into a time-varying current with a known frequency and magnitude; this time-varying current, when applied to an inductor, generates an electromagnetic field. When an inductor in air is the source of the magnetic field, the magnetic flux density B (Wb/m^2) can be calculated by

$$B = \mu_0 \mathrm{In} \tag{4}$$

where μ_0 is the permittivity of air (H/m), I is the current in the inductor (A) and n is the number of turns in the inductor [27].

A. Physics of Inductive Heating

If a material that is conductive and magnetic is perpendicular to the field lines of the inductor, part of the energy in the electromagnetic field induces an electromotive force (emf) in that material as indicated by Faraday's law of induction [27]. This law states that the *emf* (V) induced is:

$$emf = -\frac{d}{dt}\oint_s \boldsymbol{B}\cdot ds \tag{5}$$

where S is the area of the loop (m^2).

The induced emf in (5) causes eddy currents, or circulating flows of electrons, in the conductive material. This current is converted to heat via Joule heating as described in (1) and (2). This heat is used to raise the temperature of the fluid in the well.

The resistivity of the conductive material and the depth to which the current penetrates the material determine how much the heat is generated by a given induced eddy current. The skin effect defines the depth to which the induced current penetrates the material at a given frequency, f (Hz), and for given material properties. The skin depth (m) is given by

$$\delta = \sqrt{\frac{2\rho}{2\pi f \mu}} \tag{6}$$

where μ is the magnetic permeability of the material (H/m) and ρ is the resistivity (Ω·m) [26]. When the material is much thinner than the skin depth, the eddy currents are induced throughout the material, and an increase in frequency does not have an effect on the heat generated for a given magnetic field. When the material is much thicker than the skin depth, an increase in frequency decreases the skin depth, decreasing the cross-sectional area in which the eddy currents flow, increasing the temperature generated for a given magnetic field [26,27].

IV. EXPERIMENTAL METHODS

A. Temperature Measurement

Low-specific heat, coated wire (36 gauge) was soldered to the terminals of a resistance temperature detector (RTD) (Vishay PTS120613P11K), and it was coated with acrylic lacquer so it was impermeable to water. The RTD's surface-mount form factor (0.5mm x 3.2mm x 1.6mm) enabled it to be fully submerged in the water in the well to directly measure the water temperature. The RTD resistance, which can be converted to a temperature that is accurate to ±0.53°C, was measured using a digital multi-meter.

B. Resistive Heating of Fluid in Cartridge Well

Plastic cartridges were injection molded by Proto Labs, Inc. from a high impact Polystyrene (HIPS) material with the external dimensions and well dimensions described in the resistive heating simulation description. The 4mm diameter resistor cavity was drilled in each cartridge after molding. The heating resistor, a 1-kΩ 1206 surface mount resistor (Stackpole Electronics RNCS1206BKE1K00), with

wires soldered to each pad was placed at the top of cavity, touching the surface closest to the well. As in the simulation, three different thicknesses (l_g) of HIPS between the bottom of the well and the heating resistor were tested: 600, 300, and 100 µm). After the heating resistor was in place, the remainder of the cavity was filled with a high-density, ceramic-based thermal compound (Céramique, Arctic Silver). Photographs of the modified cartridge are shown in Figure 5.

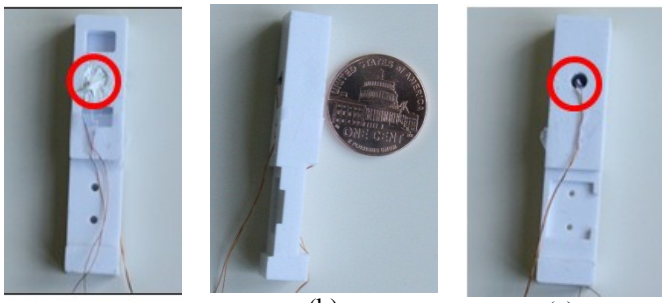

(a) (b) (c)

Figure 5. Cartridge modified for resistive heating experiments. (a) Bottom view of cartridge, showing the cavity for the resistor and thermal compound (shown inside the circle). (b) Side view. (c) Top view, showing well with RTD temperature sensor (shown inside the circle).

The well was filled with 35µL of water with the RTD fully submerged. A 15V potential was applied across the heating resistor with a DC regulated power supply (BK Precision 1670A). Temperature was measured with the RTD and a digital multimeter in resistance measurement mode; temperatures were recorded every 30 seconds during the experiment.

C. *Inductive Heating of Fluid in Cartridge Well*

1) *Signal generation circuit:*

The circuit designed for to convert a DC voltage to an AC voltage and to drive the inductor to generate the magnetic field for inductive heating is shown in Figure 6. A Wien-circuit oscillator creates a sinusoidal signal that is used as an input for the IRF630 MOSFET, which drives the inductor with the source current signal, *I* in (4). This oscillator was designed to generate frequencies from 2 kHz to 12 kHz, when tuned with the potentiometers. The inductor is the load of the MOSFET as shown in Figure 6. A 5V V_{cc} produced current of 280 mA at 2.8 kHz; V_{cc} was adjusted to maintain a roughly constant current when the frequency (and therefore the load) was changed. For more detail the switching topologies refer to [31].

2) *Inductor*

As described in (4), the inductor transforms the time-varying current from the source into a magnetic field at the same frequency, with amplitude defined by the inductor characteristics (shape and material) and the magnitude of the applied current. The inductor specifications are as follows: inductor diameter (17mm) was selected to be as small as possible while fitting the entire cartridge inside as shown in Figure 7; this concentrates the magnetic field in the well as much as possible. The number of turns (100) multiplied by the applied current *I* and the permeability of air μ_0 will define the magnitude of the magnetic flux *B* inside the inductor. The wire diameter for the inductor (0.14mm) was selected to be as thin as possible while accommodating the ~300mA driven through it in the experiments. This system is diagrammed in Figure 7, and a photograph of the inductor, the cartridge, and the conductive material is shown in Figure 8.

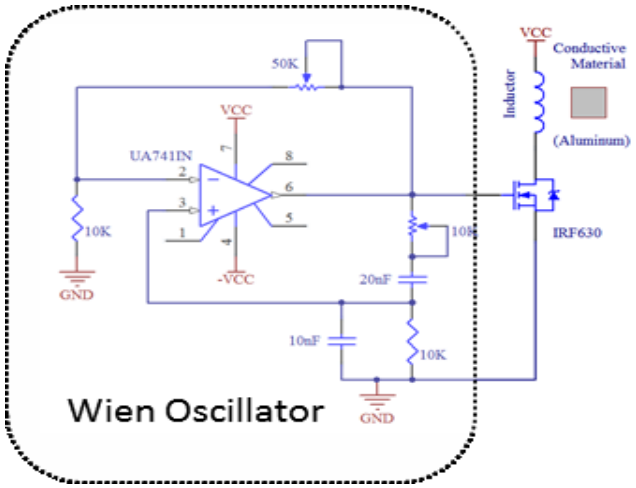

Figure 6. Circuit for driving the inductor for heating the conductive material in the well. The Wien oscillator generates a sinusoidal signal, which switches the source voltage of the IRF630 MOSFET, generating the source current, I, that flows through the inductor. The inductor generates a magnetic field, which induces eddy currents in the conductive material.

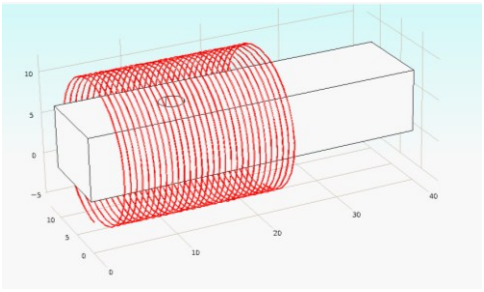

Figure 7. Drawing of inductive heating system. The cartridge was placed inside the inductor, and the conductive material was placed inside the well, perpendicular to the magnetic field.

3) *Conductive Material:*

A 0.08 mm thick aluminum sheet with dimension of 4mm x 6mm was used as the conducting material. This was placed in the well perpendicular to the magnetic field. A photograph of this material outside the well is shown in Figure 8.

4) *Experiment*

The cartridge with the conductive material in the well was placed inside the inductor with the well centered in the inductor. The oscillator was tuned to drive the inductor at four different frequencies, and at each frequency V_{cc} was adjusted to keep the current flowing through the inductor relatively constant.

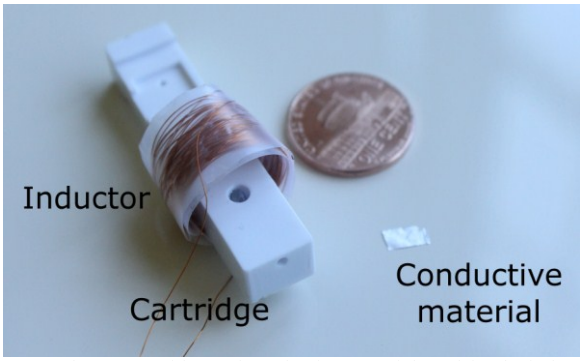

Figure 8. Inductor, cartridge and conductive material used for the inductive heating experiment. During the experiment, the well was at the center of the inductor as shown in Figure 7, and the conductive material was inside the well, perpendicular to the magnetic field.

D. Calculation of Efficiency

The calculated efficiency presented in this paper is based on the actual change in temperature of the water and not the heat generated in the conductive material as in previous works [29,30].

The heat, Q (J), transferred to the water in the well is

$$Q = C_p \cdot m \cdot dT \quad (7)$$

where Cp is the heat capacity of the water (4.185J/(g·K)), m is the mass of the water (3.5×10^{-2}g for 35µL of water), and dT is the change in temperature (K). The efficiency is calculated by dividing Q (J) by the energy input into the heater circuits:

$$\eta = \frac{Q}{P_{input}\cdot(t_1 - t_0)} \quad (8)$$

where P_{input} is measured by the power supply used to drive the electronic circuits used in these experiments, t_1 is the time where temperature reached 10°C and t_0 is the time power to the heater was initiated. A 10°C increase in temperature is used to measure the efficiency of heating in each experiment.

V. Results

A. Simulated Resistive Heating of Fluid in Cartridge Well

The simulation was run for 300 seconds with a one second interval. Results (shown with experimental results in Figure 10, suggest that 35℃ can be reached in 64s, 96s, and 120s, for the 100 µm, 300 µm, and 600µm values of l_g, respectively.

Figure 9 shows the distribution of temperatures in the cartridge, resistor, thermal paste, and water for a design with a 600µm value of $\boldsymbol{l_g}$. The transparency feature on COMSOL is turned on so it is possible to see the internal geometries. At 300 seconds, the resistor and the conductive paste reached a maximum of 55℃, while the water well heated to 39℃. The model indicates that a decreasing $\boldsymbol{l_g}$ increases efficiency, decreasing the time required to reach a given temperature.

B. Measured Resistive Heating of Fluid in Cartridge Well

Experimental readings of the temperature of the water in the cartridge well are plotted with the simulated results in Figure 10. Experimental and simulated values of efficiency for heating the water in the cartridge well 10°C above start temperature are shown in Table 2. The power dissipated in the 1kΩ resistor at 15V is 0.225W in both the simulation and the experiment. Like the simulation result, the experimental values show that a decrease in $\boldsymbol{l_g}$ increases efficiency and decreases the time required to reach a target temperature.

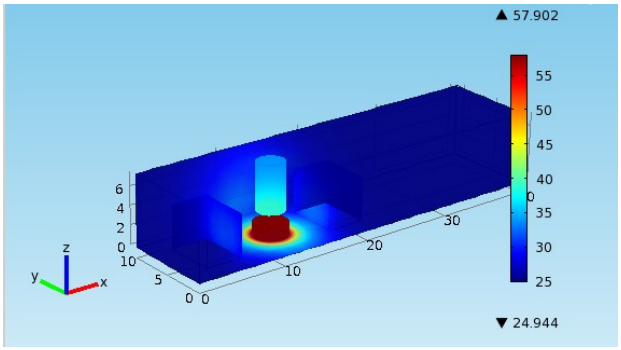

Figure 9. COMSOL simulation showing the distribution of temperatures in the cartridge, resistor, thermal paste, and water for after resistively heating a cartridge with a 600µm value of $\boldsymbol{l_g}$.

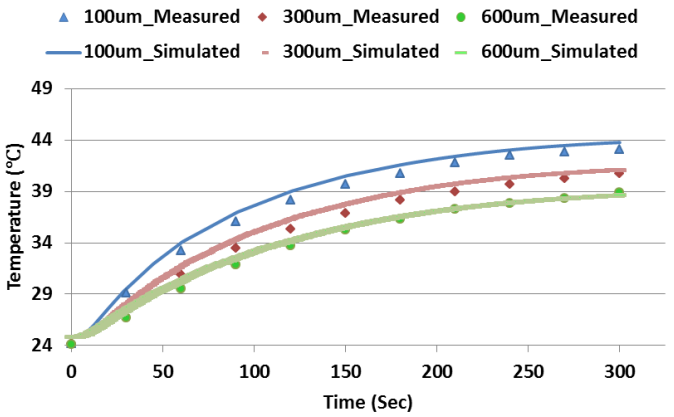

Figure 10. Measured and simulated temperatures of fluid in the cartridge well vs. time for different values of $\boldsymbol{l_g}$ (values shown in legend) during resistive heating.

TABLE II
CALCULATED EFFICIENCY OF INCREASING TEMPERATURE OF FLUID IN CARTRIDGE WELL BY 10 °C WITH RESISTIVE HEATING WITH DIFFERENT VALUES OF l_g BASED ON EXPERIMENTAL AND SIMULATED RESULTS

$\boldsymbol{l_g}$ (µm)	Experimental Efficiency (%)	Simulated Efficiency (%)
100	9.81	11.6
300	6.73	8.64
600	5.18	6.25

C. Measured Inductive Heating of Fluid in Cartridge

The cartridge was heated inductively at four different frequency/current combinations: 3.8 kHz at 270 mA, 4.6 kHz at 290 mA, 10 kHz at 157 mA, and 10 kHz at 290 mA. The same cartridge, well, and conductive material were used for all four experiments. During each experiment, temperature was measured every 30s.

Data of temperature vs. time are shown for each inductive heating experiment in Figure 11 and the efficiency calculated for heating the water in the cartridge well 10°C above start temperature are shown in Table 3.

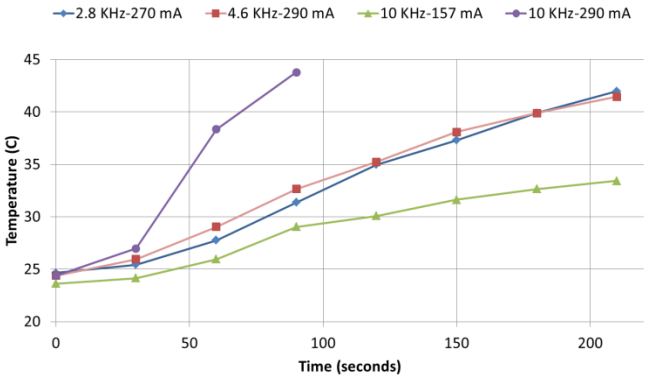

Figure 11. Measured temperatures of fluid in the well vs. time during cartridge inductive heating. while driving the inductor with different frequencies and currents.

TABLE III
CALCULATED EFFICIENCY OF INCREASING TEMPERATURE OF FLUID IN CARTRIDGE WELL BY 10 °C WITH INDUCTIVE HEATING AT DIFFERENT SOURCE FREQUENCIES AND SOURCE CURRENTS BASED ON EXPERIMENTAL RESULTS

Source Frequency (kHz)	Source Current (A)	Temperature Change (°C)	Efficiency (%)
2.8	0.27	10.33	1.57
4.6	0.29	10.84	1.44
10	0.16	9.81	0.87
10	0.29	11.37	1.55

VI. DISCUSSION

A. *Resistive Heating*

The results indicate that low-cost surface mount resistors can be used to heat 35µL fluid volumes in injection-molded plastic cartridges.

While there is good agreement for resistive heating between the experimental and simulated results, the temperature increases 1.18 times faster in the simulation than in the experimental results. This discrepancy is likely due to the fact that the heat transfer coefficient was not included in the simulation, which kept the water warmer than in the experimental case, where there was some heat transfer from water to air.

Both the experimental and simulated results show that a decrease in l_g decreases the time needed to reach a given temperature, and increases the efficiency. This indicates that, were this design to be manufactured, the thickness of plastic between the heating resistor and the well must be kept as small as can be reproducibly manufactured.

The agreement between the experiment and the model indicates that the model is accurate and can be modified to test other design variables for resistive heating.

B. *Inductive Heating*

The results show that it is possible to heat 35µL fluid volumes in a controlled fashion using magnetic induction. This is promising for bioassay applications for which it is beneficial not to have electrical contact between the power source and the heater, for which localization of heating is required, and/or for which the size of the heat source is restricted due to small reagent volumes

The ability to change the power delivered by changing the frequency with constant current enables fine control of temperature. The frequency could be increased when a fast ramp in temperature is required, and decreased when the temperature does not need to change as quickly.

There was not a significant change in the energy transferred to the solution when the frequency was changed from 2.8kHz to 4.6kHz with approximately constant current. However, when the frequency was increased to 10kHz, there was a significant increase in energy delivered. In these experiments, the thickness of the conductive material (0.08mm) was below the skin depth for the applied frequencies (0.8mm at 10kHz to 1.5mm at 2.8kHz), and the conductive material used (aluminum) is a paramagnetic material, which has a complex magnetic susceptibility. As the conductive material thickness approaches one tenth of the skin depth, the complex portion of the susceptibility begins to have a significant effect on the impedance of the conductive material, increasing the energy dissipated as heat, dramatically increasing the efficiency of the inductive system. In the generator, increasing the frequency decreased the efficiency of inductive heating, but by optimizing the design of the inductor for the most efficient frequency, losses could be reduced in both components. Alternatively, the thickness of the conductive material could be increased to improve the energy delivered at frequencies where the existing generator has low losses.

Previous publications of inductive heating of bioassay reagents [29,30] were designed for PCR and a time constant greater than 5°C/s. To achieve this time constant, the thermal mass of the heater was much greater than that of the reagents being heated. Alternatively, in the work presented in this paper, the thermal mass of the heater is significantly less than that of the assay reagents being heated, improving efficiency for an isothermal bioassay, for which the time constant is not critical, and enabling operation with a small, portable battery.

C. *Future Work*

This work explored heating the fluid in the cartridge well; the next step is to add a closed loop to maintain a specific temperature within a required accuracy for a specified period of time. Different applications require different accuracies, from ±1°C to ±5°C. Because the diagnostic isothermal applications will involve temperature regulation above room temperature, only a heating element and a temperature sensor are required for closed-loop temperature control. Optimizing the temperature control system for the application will involve a tradeoff between heating efficiency (with minimal heat dissipation to the surroundings) and thermal response time for cooling (with more heat dissipation to the surroundings). Several devices for other applications with microliter to milliliter-scale chambers and operating temperatures from 30-50°C have temperature control precision better than ±1°C [32-34].

For both heating methods, the efficiency can be further optimized for battery-operated, point-of-care bioassay

applications. The surface-mount resistive heater efficiency can likely be improved by optimizing the size and position of the resistor, and possibly by including additional surface-mount resistors arrayed around the well rather than only below the well. The inductive heating system efficiency can be improved by using different conductive materials, conductive materials with different form factors, and inductors with different geometries. For example, the thickness of the conductive material can be increased to achieve a conductive material thickness to skin depth ratio that optimizes heating efficiency for a given cartridge geometry and material.

VII. Conclusion

This work describes two low-cost methods for heating reagents in disposable bioassay cartridges. A model for simulation of heating with a surface-mount resistor was presented and validated with prototype cartridges. This model can be extended to optimize the size and orientation of channels and resistors in the cartridge for maximum thermodynamic efficiency or to meet other design goals. Inductive heating of cartridge components without electrical contact was successful. While this method is less efficient than resistive heating, it can be further optimized and may be a desirable method in cases where no other electrical interface to the cartridge is otherwise required. The proposed heating technologies are flexible enough that they are compatible with integration in many types of disposable cartridges for *in vitro* diagnostics, environmental monitoring, and other applications.

Acknowledgment

The authors wish to acknowledge the valuable discussions with Dr. Antonio J. Ricco.

References

[1] *Rapid HIV Tests: Guidelines for Use in Testing and Counseling Services in Resource-Constrained Settings,* World Health Organization, Geneva, Switzerland, 2004.

[2] HIV Assays: Operational Characteristics: Report 16 Rapid Assays, World Health Organization, Geneva, Switzerland, 2009.

[3] *Malaria Rapid Diagnosis: Making it Work; Meeting Report*, World Health Organization, Geneva, Switzerland, 2003.

[4] A. Calmy et al., "HIV viral load monitoring in resource-limited regions: optional or necessary?," Clin Infect Dis, vol. 44, no. 1, pp. 128-34, 2007.

[5] S. A. Fiscus et al., "HIV-1 viral load assays for resource-limited settings," PLoS Med, vol. 3, no. 10, p. e417, 2006.

[6] M. Urdea et al., "Requirements for high impact diagnostics in the developing world," Nature, vol. 444 Suppl 1, pp. 73-79, Nov. 2006.

[7] M. L. Schito, M. P. D'Souza, S. M. Owen, and M. P. Busch, "Challenges for rapid molecular HIV diagnostics," The Journal of Infectious Diseases, vol. 201 Suppl 1, pp. S1-6, Apr. 2010.

[8] C. Zhang, J. Xu, W. Ma, and W. Zheng, "PCR microfluidic devices for DNA amplification," Biotechnology Advances, vol. 24, no. 3, pp. 243-284, Jun. 2006.

[9] P. R. Selvaganapathy, E. T. Carlen, and C. H. Mastrangelo, "Recent progress in microfluidic devices for nucleic acid and antibody assays," Proceedings of the IEEE, vol. 91, no. 6, pp. 954-975, 2003.

[10] J.L. Gerlach et al., "Developing a point-of-care multiplexed diagnostic system for low-resource settings in developing countries," presented at Molecular Medicine Tri-Conference, San Francisco, CA, March 25, 2008.

[11] P.D. LaBarrre et al., "HOT Diagnostic Technologies: Low-cost, point-of-care nucleic acid amplification using chemical heat to replace traditional heat sources," presented at 6th Annual World Health Care Congress, Washington, DC, April 12, 2009.

[12] D.S. Stevens et al., "Affordable point-of-care viral RNA specimen processing for low-resource settings," presented at AACC 42nd Annual Oak Ridge Conference, San Jose, CA, April 22, 2010.

[13] D. Tang et al., "Non-Instrumented Nucleic Acid Amplification," presented at the American Association for Clinical Chemistry 40th Annual Oak Ridge Conference, San Jose, CA , April 17, 2008.

[14] C.G. Koh, W. Tan, M. Zhao, A.J. Ricco, and Z.H. Fan, Integrating Polymerase Chain Reaction, Valving, and Electrophoresis in a Plastic Device for Bacterial Detection, *Anal. Chem*.,vol. 75, pp. 4591-4598, 2003.

[15] L. J. Kricka and P. Wilding, "Microchip PCR," Analytical and Bioanalytical Chemistry, vol. 377, no. 5, pp. 820-825, Nov. 2003.

[16] M. L. Collins et al., others, "A branched DNA signal amplification assay for quantification of nucleic acid targets below 100 molecules/ml," Nucleic acids research, vol. 25, no. 15, p. 2979, 1997.

[17] D. A. Di Giusto, W. A. Wlassoff, J. J. Gooding, B. A. Messerle, and G. C. King, "Proximity extension of circular DNA aptamers with real-time protein detection," Nucleic Acids Research, vol. 33, no. 6, p. e64-e64, 2005.

[18] M. A. Burns et al., others, "An integrated nanoliter DNA analysis device," Science, vol. 282, no. 5388, pp. 484-487, 1998.

[19] H. H. Lee, M. A. Dineva, Y. L. Chua, A. V. Ritchie, I. Ushiro-Lumb, and C. A. Wisniewski, "Simple Amplification-Based Assay: A Nucleic Acid–Based Point-of-Care Platform for HIV-1 Testing," The Journal of Infectious Diseases, vol. 201, no. 1, p. S65-S72, 2010.

[20] A. Niemz, T. M. Ferguson, and D. S. Boyle, "Point-of-care nucleic acid testing for infectious diseases," Trends in Biotechnology, vol. In Press, Corrected Proof, 2011.

[21] S. Lutz et al., "Microfluidic lab-on-a-foil for nucleic acid analysis based on isothermal recombinase polymerase amplification (RPA)," Lab on a Chip, vol. 10, no. 7, pp. 887-893, Apr. 2010.

[22] D. Erickson and D. Li, "Integrated microfluidic devices," Analytica Chimica Acta, vol. 507, no. 1, pp. 11-26, Apr. 2004.

[23] C. M. Sames, *A Pocket-book of Mechanical Engineering*, Robert Drummond, 1906.

[24] F.P. Incropera, D.P.DeWitt, Introduction to Heat Transfer, 2nd Edition, School of Mechanical Engineering, Purdue University, New York, John Wiley and Sons, 1990.

[25] Céramique Material Property Specifications. Retrieved April 13, 2011, from http://www.arcticsilver.com/ceramique.htm

[26] F. Fiorillo and I. Mayergoyz, *Characterization and Measurement of Magnetic Materials (Electromagnetism)*. Academic Press, 2005.

[27] M. Iskander, *Electromagnetic Fields and Waves*. Waveland Press, 1992.

[28] S. V. Kulkarni and S. A. Khaparde, *Transformer Engineering: Design and Practice*, 1st ed. CRC Press, 2004.

[29] D. Pal, K. N. Mohan, H. S. Chandra, and V. Natarajan, "A power-efficient thermocycler based on induction heating for DNA amplification by polymerase chain reaction," *Rev. Sci. Instrum.*, vol. 75, no. 9, 2004.

[30] D. Pal and V. Venkataraman, "A portable battery-operated chip thermocycler based on induction heating," *Sensors and Actuators A: Physical*, vol. 102, no. 1-2, pp. 151-156, Dec. 2002.

[31] "Induction Heating System Topology Review AN9012." Fairchild semiconductor, 2010.

[32] T. Yamamoto, T. Fujii, and T. Nojima, "PDMS-glass hybrid microreactor array with embedded temperature control device. Application to cell-free protein synthesis," Lab on a Chip, vol. 2, no. 4, pp. 197-202, Nov. 2002.

[33] S. Petronis, M. Stangegaard, C. B. V. Christensen, and M. Dufva, "Transparent polymeric cell culture chip with integrated temperature control and uniform media perfusion," BioTechniques, vol. 40, no. 3, pp. 368-376, Mar. 2006.

[34] M. N. H. Z. Alam, D. Schäpper, and K. V. Gernaey, "Embedded resistance wire as a heating element for temperature control in microbioreactors," Journal of Micromechanics and Microengineering, vol. 20, no. 5, p. 055014, May. 2010.